

Supporting Information

Tobin *et al.* 10.1073/pnas.0707057105

SI Materials and Methods

Human Subjects. We undertook 3D facial scanning (as previously described) in 83 patients (all Caucasian) with BBS (diagnosed according to criteria in ref. 7) following consent and ethical approval. Patients were matched for age, sex, and race to 230 Caucasian controls. Following manual landmarking, all dense surface models were computed using software developed in-house.

Mouse Skull Scanning. Major superficial muscles of the head were grossly dissected and then fixed overnight in 95% ethanol. The skulls were then transferred to 2% KOH for 7 days, refreshing the KOH solution daily. Finally, they were dehydrated in 95% ethanol for 48 h and air dried before scanning. 3D scans of 31 *Bbs4*^{-/-}, 30 *Bbs4*^{+/-}, and 20 wild-type live adult mice were obtained following a light anesthetic (Avertin), and their fur was painted with a cornstarch and water mixture to create a white reflective surface.

The mice were placed in the Cyberware (Monterey, CA) Desktop 3D scanner. 3D scans of skulls from *Bbs6* null mice were performed using a Roland (Irvine, CA) LPZ-1200 desktop laser scanner.

Zebrafish Studies. We designed antisense MOs (Gene Tools, Philomath, OR) directed against the start ATG of *bbs4*, *bbs6*, and *bbs8* (sequences available upon request). We were able to fully rescue the effects of each MO by coinjecting with full-length mRNA, thus confirming specificity of the morpholinos. To visualize the cartilage, embryos were stained with Alcian Blue in whole-mount according to standard protocols (36). Chondrocrania were flat-mounted on glass slides and imaged. Standard protocols were used for *in situ* hybridization. Probes used were as follows: *ptc1*, *pax6a*, *dct*, *crestin*, *foxd3*, *sox10*, and *phox2b*.

Cell Transplantations. Sox10:eGFP embryos were coinjected with control or *bbs8* MO and 10 kDa of rhodamine dextran (Invitro-

gen). At 4 hpf, 20–30 cells were taken from donors and grafted into hosts. Successful transplants were screened at the 12ss, mounted in agarose, and imaged over a 4-h period to visualize migrating CNCCs.

Fluorescent Imaging of Zebrafish Embryos. Sox10:eGFP embryos were mounted in agarose and imaged live on a confocal microscope. For double immunostaining, a rabbit anti-GFP antibody (Abcam) was used to reveal Sox10:eGFP positive NCCs. Primary antibodies used were as follows: Phosphohistone H3b (Millipore), HuC/D (Invitrogen), and acetylated tubulin (Sigma). Secondary antibodies used were as follows: anti-rabbit 488 and anti-mouse 568 (Invitrogen).

FACS Sorting. Control and MO-injected Sox10:eGFP embryos were dissociated at 14 or 20ss. Cells were resuspended in L15, and GFP-positive cells were sorted on a Becton-Dickinson flow sorter. Cell death was quantified with 7AAD.

Shh Cell Assay. NIH 3T3 cells stably expressing shRNA against *Bbs8* (or control shRNA) were starved in low serum for 48 h, and Shh-conditioned medium (or purmorphamine) was added. Twenty-four hours later, they were transfected with a Gli-luciferase construct and *Renilla* (Promega, Madison, WI). Luciferase assay was performed the following day (Promega). For Gli3 Western blots, purmorphamine was added to shRNA-knockdown and control cells. Cell lysates were probed with an anti-Gli3 antibody (Santa Cruz Biotechnology).

In Vitro Scratch Wound Healing Assay. NIH 3T3 and primary fibroblasts taken from *BBS8*^{-/-} patients, were seeded onto coverslips, and were grown to confluence. Cells were starved in low serum and then scratched with a sterile pipette tip. Cells were fixed at 0, 6, 24, and 48 h after the scratch and stained using Phalloidin (Invitrogen) and DAPI.

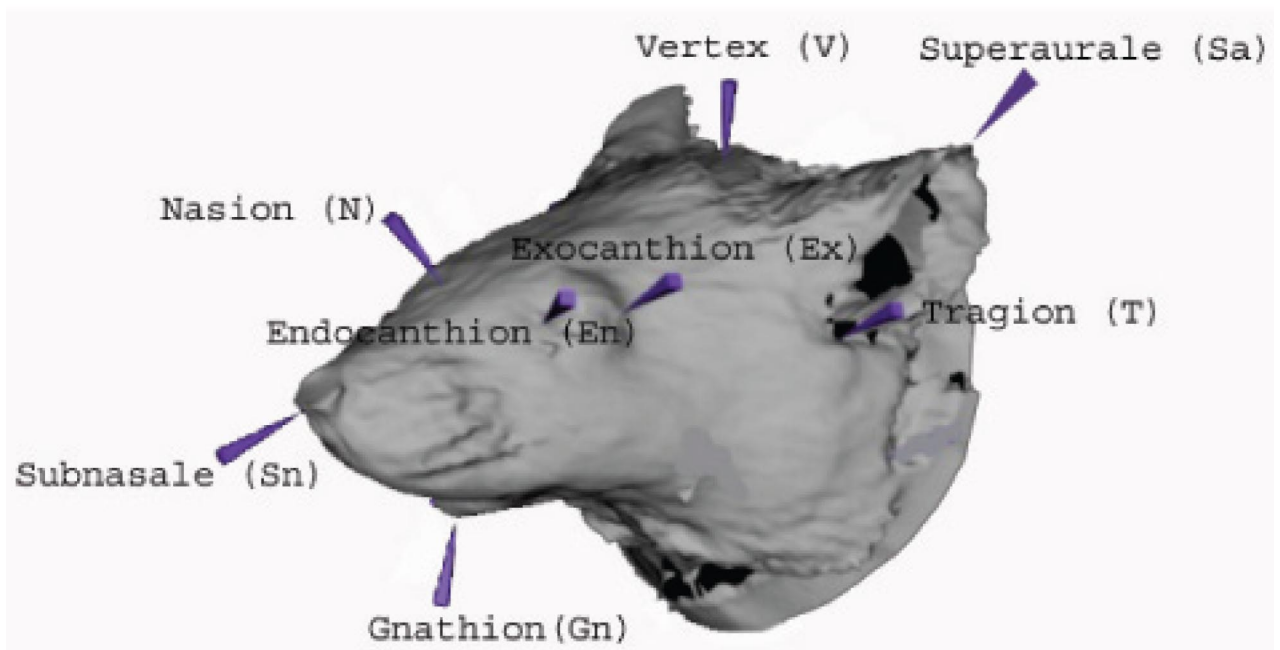
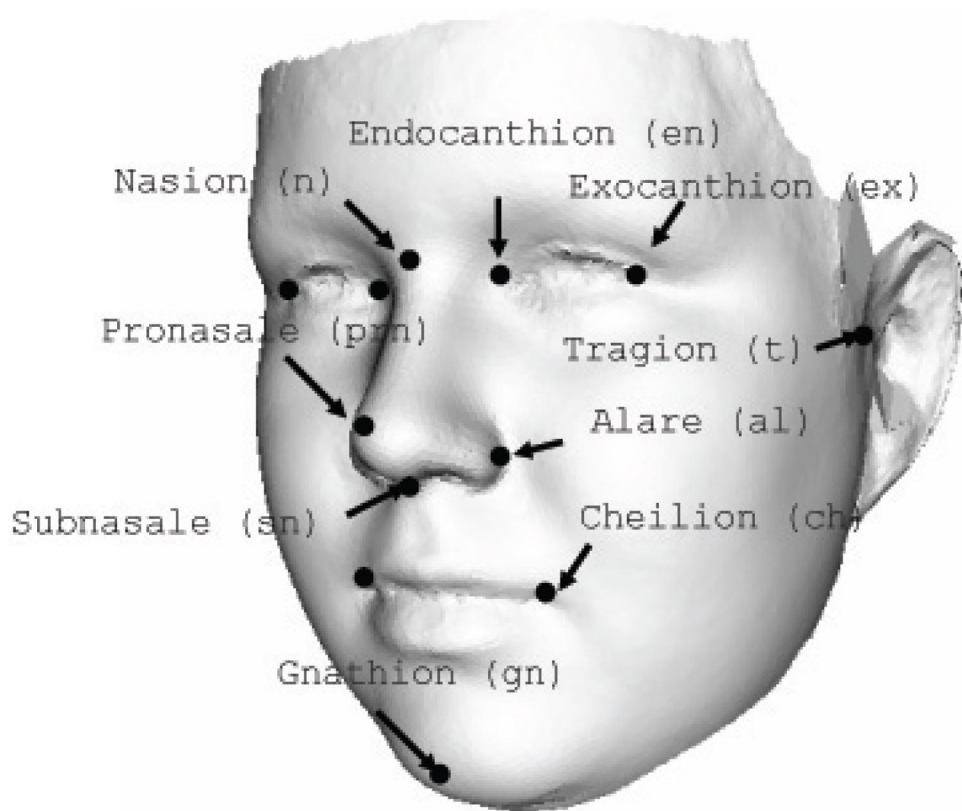
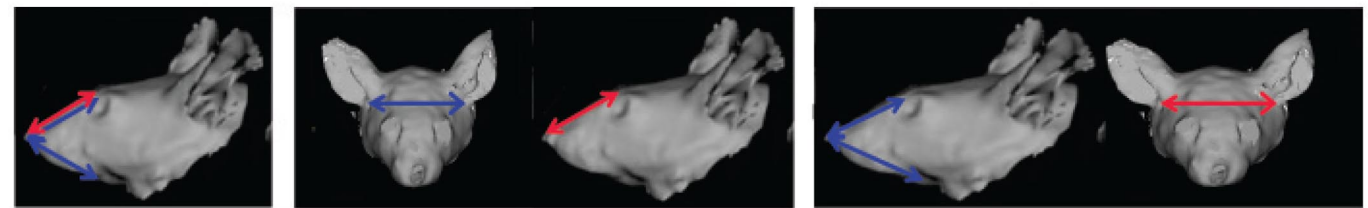
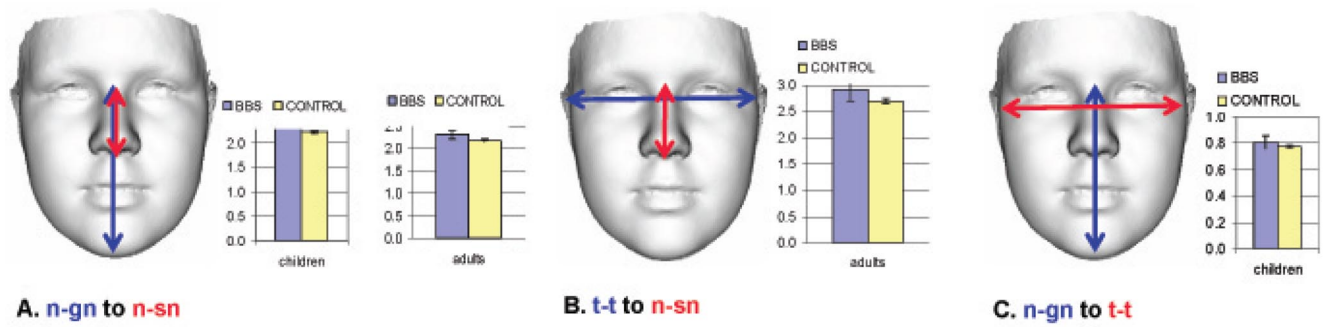


Fig. S1. Annotated surface landmarks in humans and mice.



D. (n-sn+sn-gn) to n-sn **E. t-t to n-sn** **F. (n-sn+sn-gn) to t-t**

Fig. S2. Significant landmark ratios in humans and *Bbs4* mice. Significantly changed landmark ratios are illustrated in *A*, *B*, and *C* for humans and the corresponding ratios in mice are illustrated in *D*, *E*, and *F*. (*A*) The vertical measure nasion-gnathion (n-gn) in proportion to mid-face height (n-sn) was larger in both BBS children ($P < 0.01$) and BBS adults ($P < 0.01$) compared with the controls. (*B*) The mid-face width, the tracion-tracion (t-t) measure relative to mid-face height (n-sn), is also larger in adults ($P < 0.01$) and almost so in children ($P = 0.07$). (*C*) In addition, the vertical measure n-gn in proportion to mid-face width (t-t) is larger in children ($P < 0.05$) but not in adults. (*D*) In mutant mice, the equivalent of the human n-gn measurement (n-sn + sn-gn) in relation to the n-sn length was larger in *Bbs4*-null mice ($P < 0.01$). (*E*) Similar to humans, the mid-face width (t-t) to mid-face height (n-sn) ratio is larger in null animals than their wild-type counterparts ($P < 0.01$). (*F*) In contrast to the human n-gn to t-t ratio, the null mice had a significantly smaller relationship ($P < 0.01$).

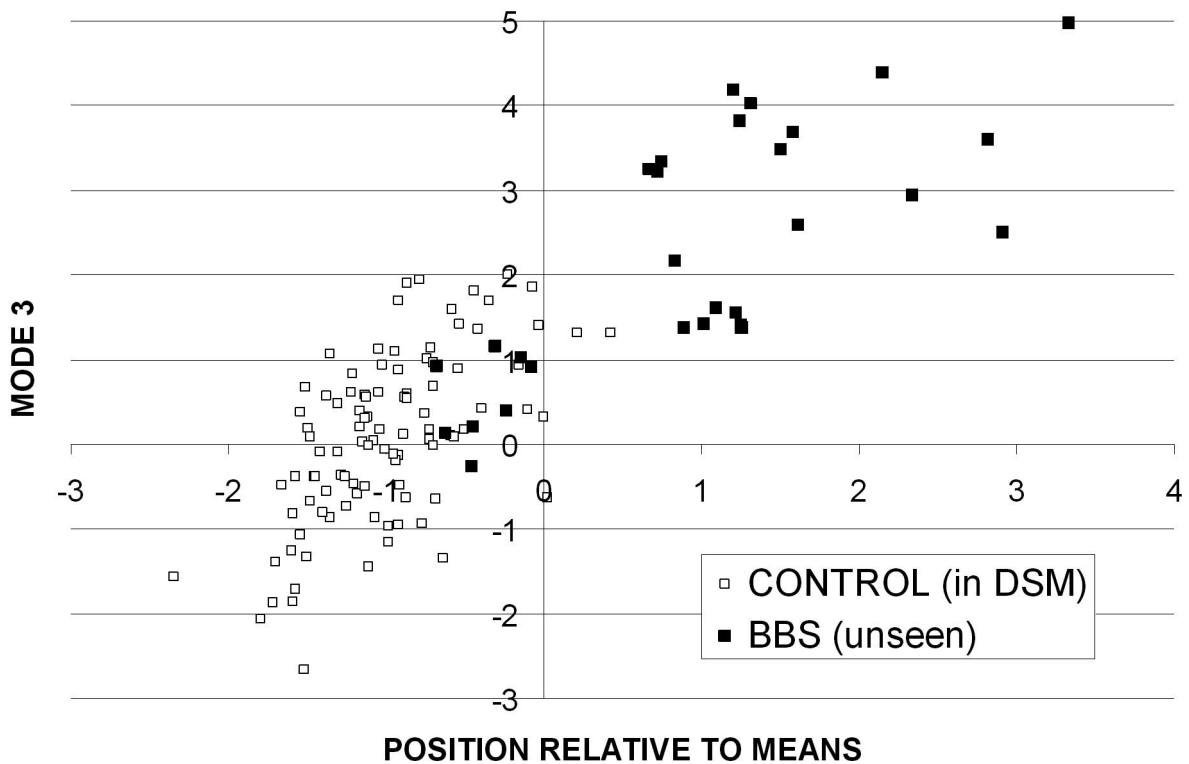


Fig. S3. Scatter plot of control-BBS classification position against PC3 of a DSM for the full face of child controls only. The BBS children’s faces were introduced unseen into a DSM for face shape computed for control children only. The PC3 scores for the faces of the combined groups was found to correlate strongly with classification position in terms of closest mean (Pearson Product Moment, 0.81). The face variation described by PC3 involves mid-facial flatness and mild retrognathia.

anti-sense



sense



Fig. S4. *bbs8* expression pattern in zebrafish. *In situ* hybridization showing ubiquitous expression of *bbs8* in the 24 hpf embryo with high levels in the eye and brain.

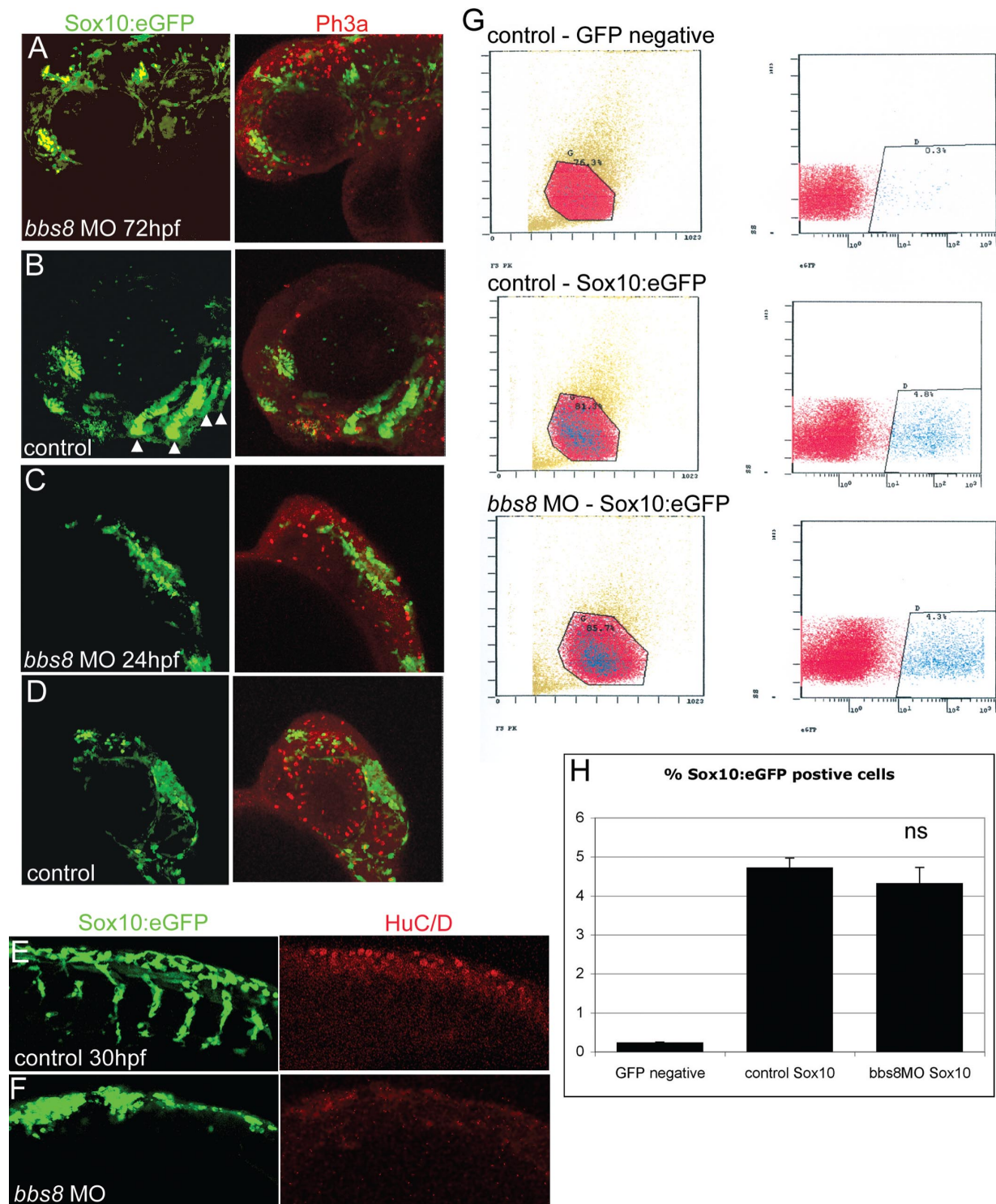


Fig. S5. Assessment of proliferation, cell death, and differentiation in *bbs8* morphant NC. (A and B) Expression of Sox10:eGFP in 72 hpf zebrafish shows a lack of pharyngeal arches in morphants relative to controls (arrowheads in B). Also, the number of proliferating Sox10:eGFP-positive cells shown by Ph3 staining (in red) is not different between control and morphant. (C and D) Sox10:eGFP expression in the head of 24 hpf fish showing the lack of migration in *bbs8* morphants. Ph3 staining again shows no difference in the amount of proliferation in the crest cells despite less proliferation in cells of the brain. (E and F) Sox10:eGFP cells migrating into the trunk at 30 hpf do not inappropriately differentiate into neurons in the *bbs8* morphants as revealed by HuC/D immunostaining (in red). (G and H) FACS plots (G) of embryos show that control and morphant Sox10:eGFP embryos have similar proportions of neural crest cells (H), indicating that proliferation of the NCCs is not affected in the morphants.

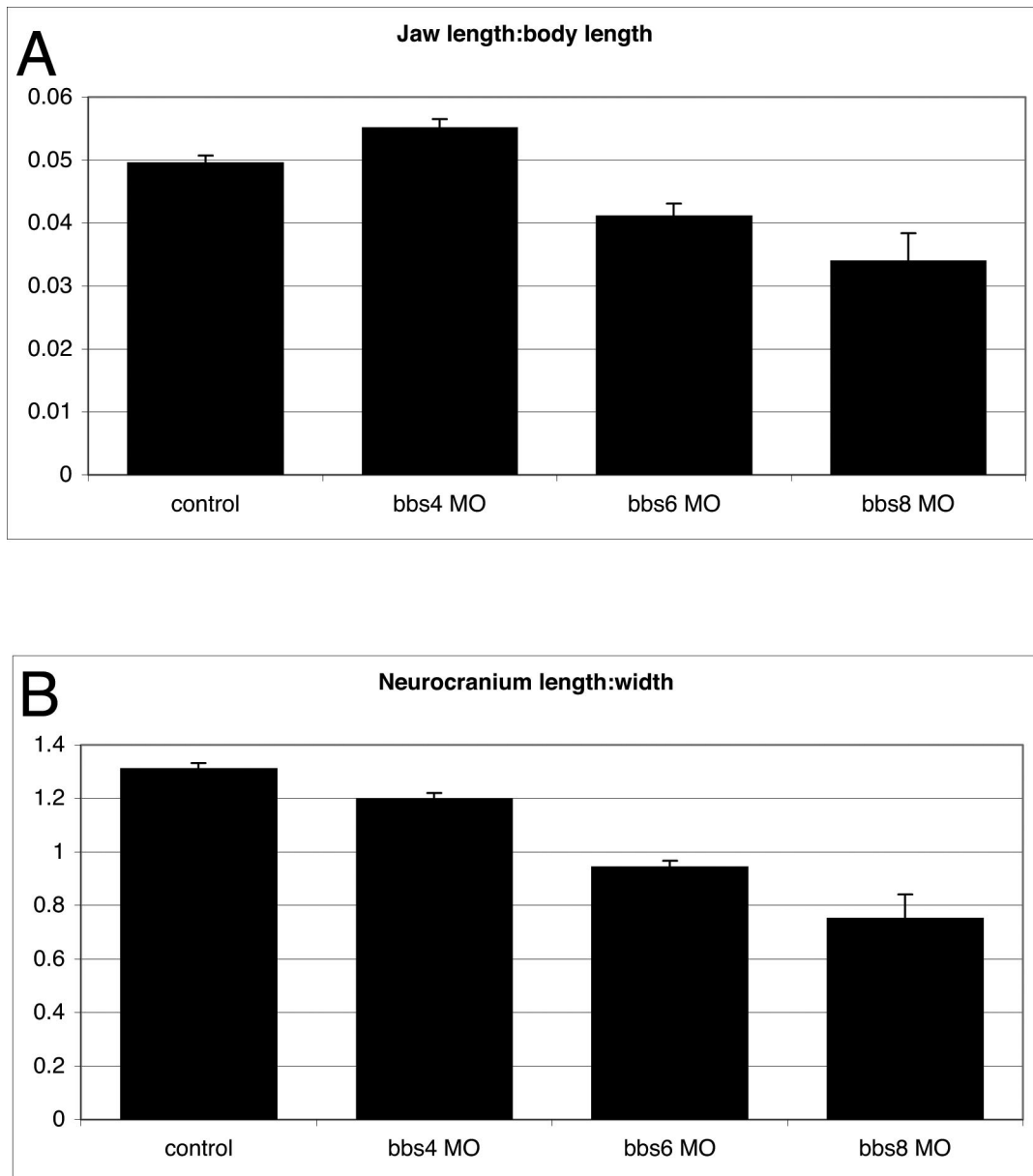


Fig. S6. Fish ANC measurements. These were reduced in morphants to a similar degree as the reduced skull length when compared with controls. This implies that the shortened ANC is independent of any CE defects. (A) Graph showing an increased ANC length to body length ratio in *bbs4* morphants due to shortening of their body axis but a relatively normal ANC length. This ratio is reduced significantly in *bbs6* and *bbs8* morphants, suggesting that the reduced ANC length is not simply due to a reduced body axis length. (B) Ratios of ANC length:width show an increasing reduction in *bbs4*, *bbs6*, and *bbs8* morphants, respectively, indicating a shorter and wider chondrocranium.

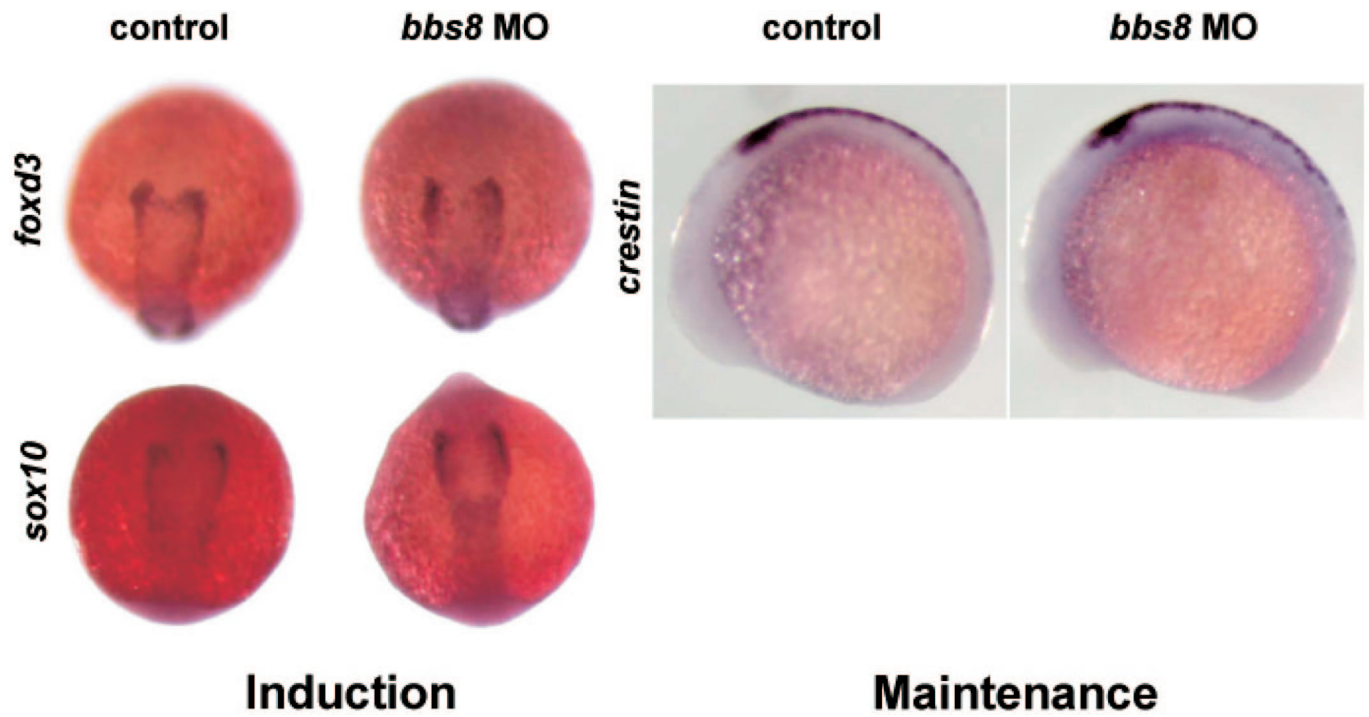


Fig. S7. Expression pattern of neural crest markers. Expression of *sox10* and *foxd3* were normal, proving that NCC induction was normal at 5 somite stage. Normal expression of *crestin* at 12 somite stage indicates that NCC maintenance and proliferation are also normal in morphants.

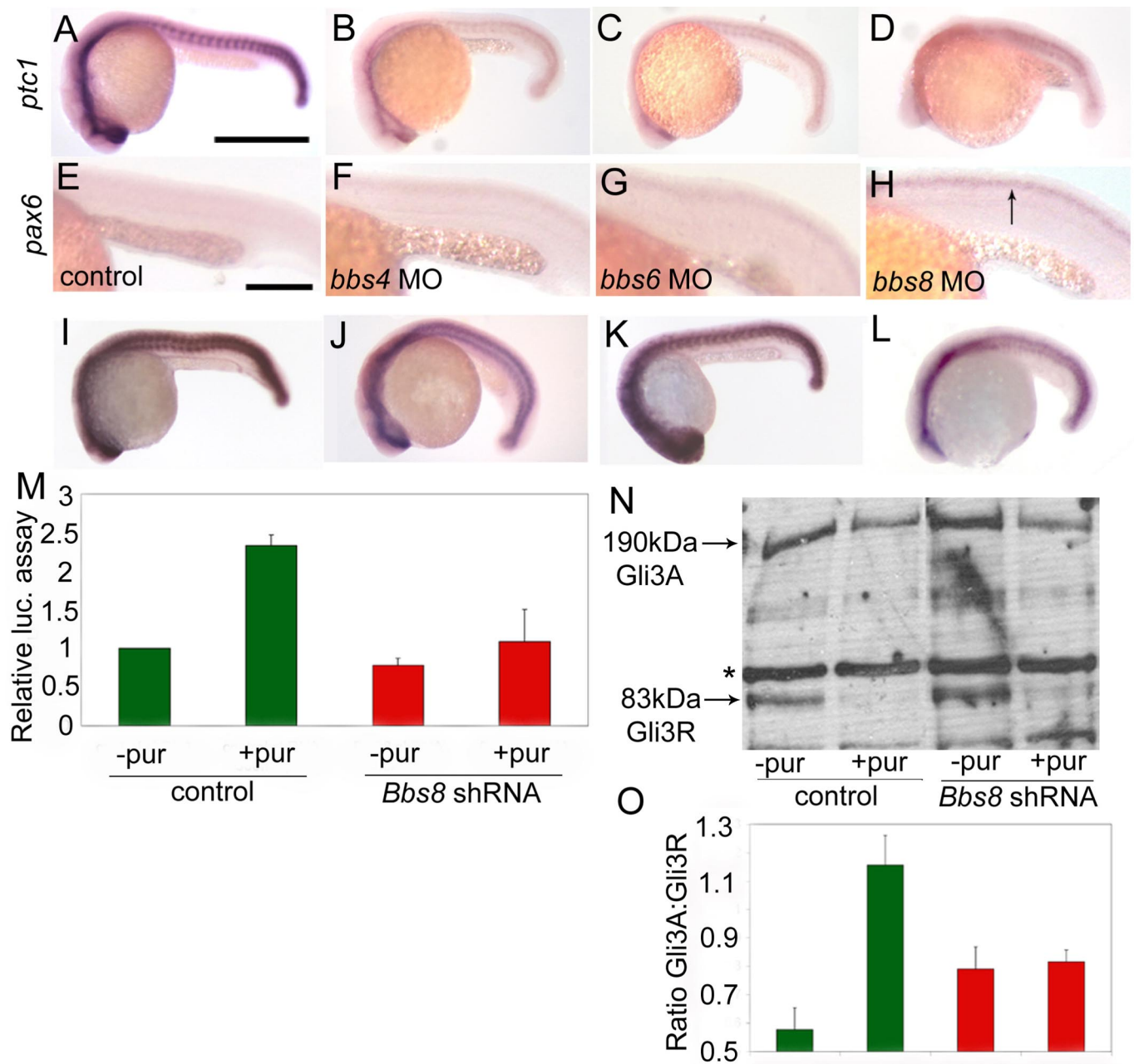


Fig. 58. Aberrant Sonic Hedgehog signaling in *bbs* morphants. (A) Expression of *ptc1*, a marker of Sonic Hedgehog pathway activity, is down-regulated in *bbs* morphants, most strikingly so in *bbs8* morphants (6D). (E and F) Conversely, *pax6*, a gene negatively regulated by Shh signaling, is up-regulated in the neural tube of *bbs8* morphants. (I) Injection of *ptc1* MO alone up-regulates expression of *ptc1* by inducing the Shh pathway. (J) Coinjection of *ptc1* MO with *bbs8* MO partially rescues this induction, implicating Bbs8 downstream of Ptc1. (K) Injection of dominant-negative PKA causes ectopic activation of the Shh pathway. (L) Coinjection with *bbs8* MO rescues this induction, suggesting that it could act downstream of PKA, likely in Gli3 transport. (M) Addition of Purmorphamine to control transfected cells induces the Gli activity by 2.5-fold. Bbs8 knockdown cells show attenuated response to Purmorphamine stimulation. (N and O) Western blot showing reduction of Gli3R in response to stimulation with Purmorphamine, resulting in a higher Gli3A;Gli3R ratio. This ratio remains unchanged when Bbs8 knockdown cells are stimulated. [Scale bars: 500 μm (A–D and I–L) and 200 μm (E–H).]

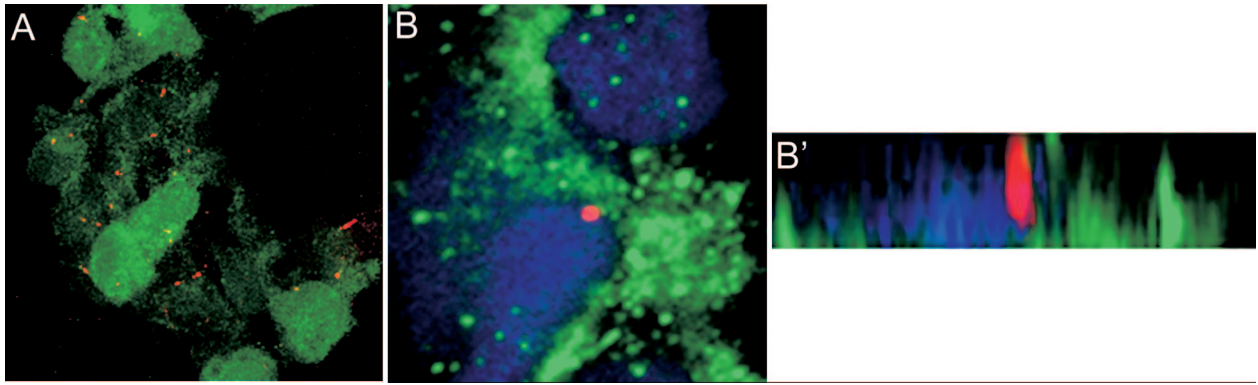


Fig. 59. NCCs bear primary cilia. (A) Neural crest cells (green) bearing cilia (arrows)(anti-acetylated tubulin, red). (B) Close-up of single cilium-bearing NCC with confocal projection showing a clear primary cilium. (B') Confocal optical section of an apical cilia emerging from a Sox10:eGFP-positive neural crest cell. The nucleus is stained in blue with DAPI.

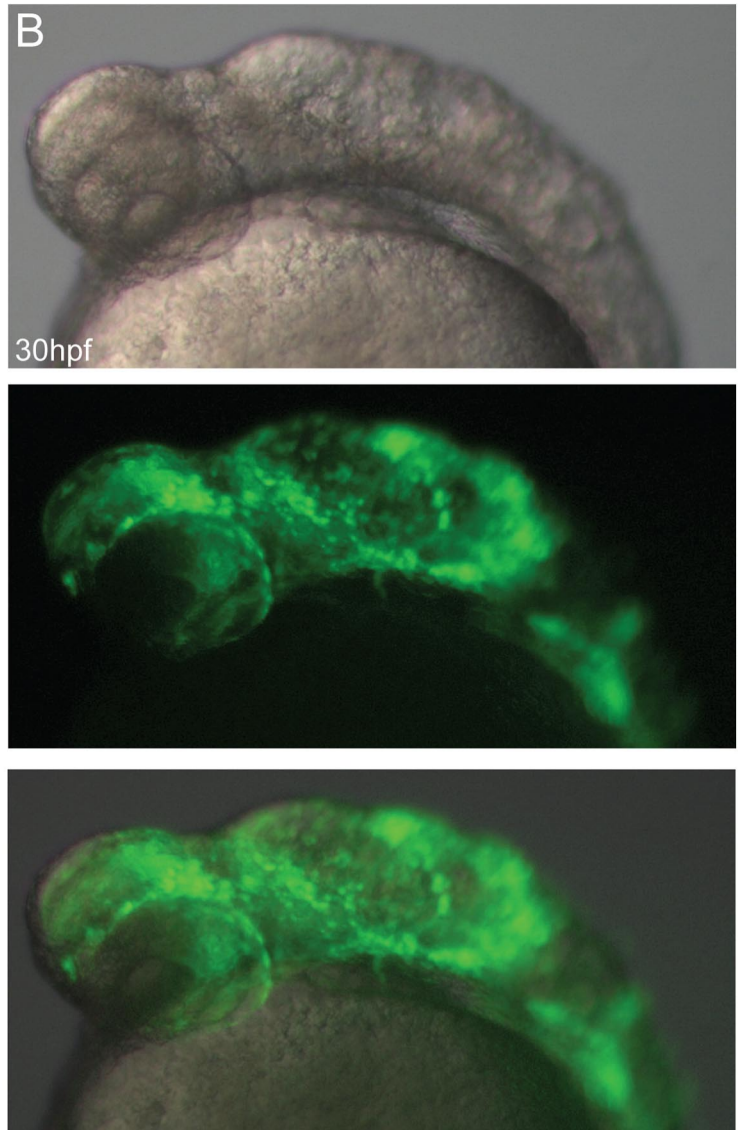
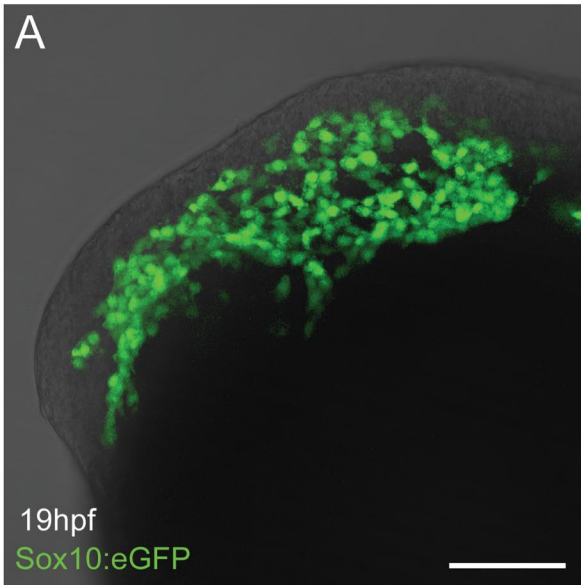
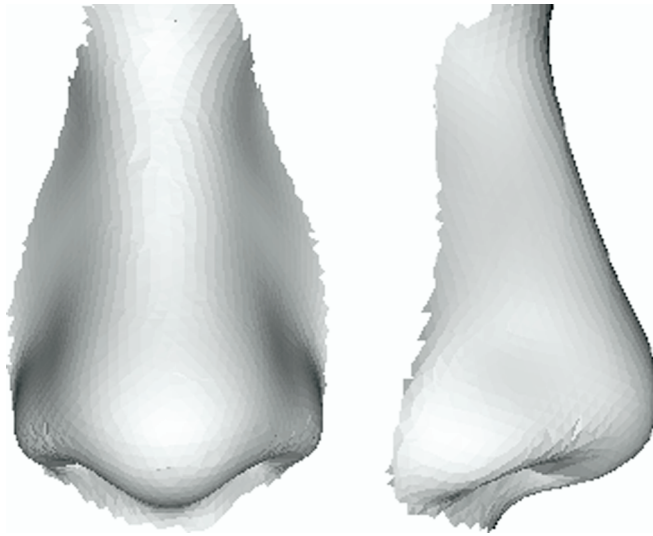


Fig. S10. Effect of cyclopamine treatment on early NCC migration. (A) Adding cyclopamine at 4 hpf causes no defect in CNCC migration at 19 hpf shown by Sox10:eGFP expression. (B) At 30 hpf, the embryos show morphological signs of Shh pathway inhibition, but CNCCs have still migrated into the head, showing that Shh signaling is not important for initial migration of cells but is critical for patterning.



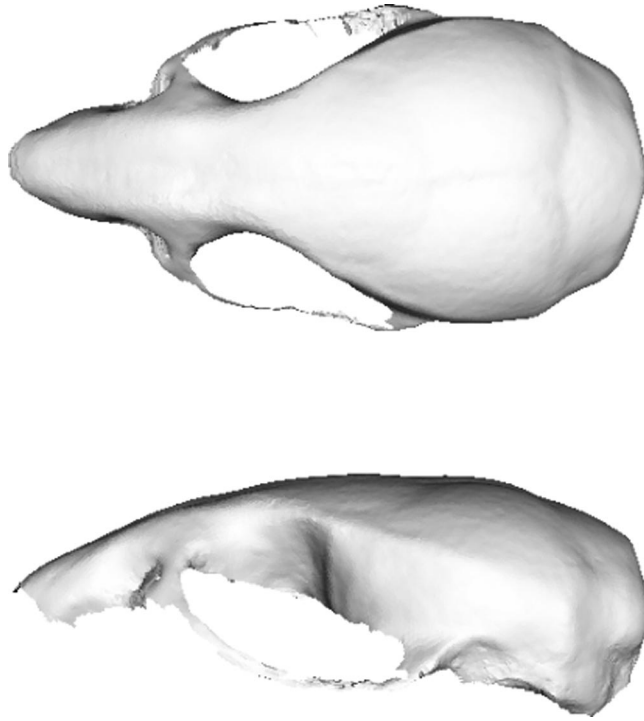
Movie S1. DSM movie clip of face shape differences between human BBS patients and controls.

[Movie S1 \(AVI\)](#)



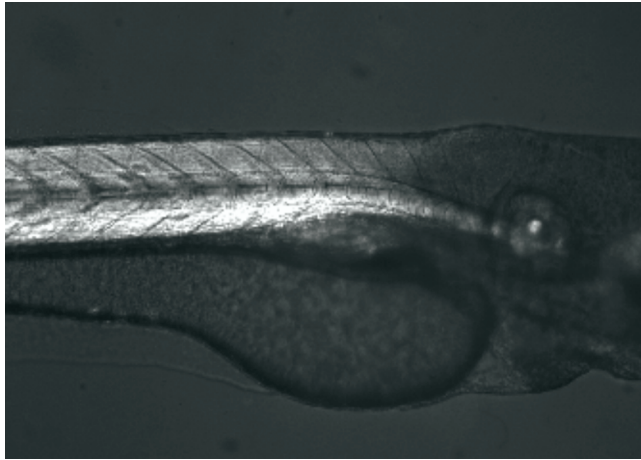
Movie S2. DSM movie clip of nose shape differences between human BBS patients and controls.

[Movie S1 \(AVI\)](#)



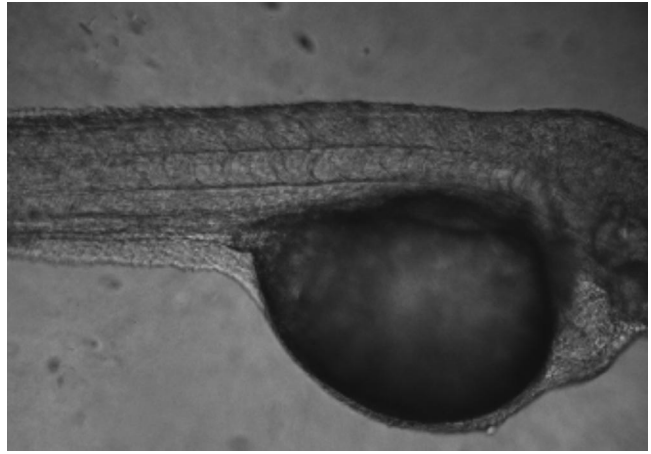
Movie S3. DSM movie clip of average facial image in *Bbs6* mutant mice, illustrating shortening of the snout and cranial vault.

[Movie S1 \(AVI\)](#)



Movie S4. Peristalsis in wild-type zebrafish at 4.5 dpf.

[Movie S1 \(MOV\)](#)



Movie S5. Lack of peristalsis in *bbs8* morphants.

[Movie S1 \(MOV\)](#)

Table S1. Accuracy of pattern recognition algorithms in classifying control and BBS patient nose shape in terms of mean area under ROC curves arising from multi-folded, randomized unseen testing

Algorithm	Mean area under roc curve		
	CM	LDA	SVM
Children	0.84	0.89	0.91
Adults	0.83	0.85	0.84

The intuitive interpretation of area under an ROC curve is the probability of correctly classifying a pair of randomly chosen subjects, one "affected" and one "unaffected." CM, closest mean; LDA, linear discriminant analysis; SVM, support vector machines.

Table S2. Mouse skull summary of mean measurements (mm) with relevant *P* values

	Skull length: width	Nasale to bregma	Frontal-squamosal intersection at temporal crest	Mandible length (superiormost point on incisal alveolar rim to mid-point and posteriormost points on mandibular condyles)
<i>Bbs6</i> homozygote (<i>n</i> = 9)	1.97	13.83	5.82	16.21
Wild-type (<i>n</i> = 7/8)	2.04	14.54	6.28	16.77
<i>t</i> test <i>P</i> value	0.02	0.004	0.04	0.04

Table S3. Measures of mandibular length and width in *bbs4* and *bbs6* morphants

	Mean mandible width	Mean mandible length
Control (WT)	156 μm	350 μm
<i>bbs4</i> morphant ($n = 8$)	207 μm ($P < 0.01$)	322 μm ($P < 0.05$)
<i>bbs6</i> morphant ($n = 6$)	198 μm ($P < 0.001$)	n/a

n/a, not available.